rf breakdown with external magnetic fields in 201 and 805 MHz cavities

R. B. Palmer, R. C. Fernow, Juan C. Gallardo, and Diktys Stratakis
Brookhaven National Laboratory, Upton, New York 11973, USA

Derun Li
Lawrence Berkeley National Laboratory, Berkeley, California 94720, USA
(Received 8 September 2008; published 12 March 2009)

Neutrino factory and muon collider cooling lattices require both high gradient rf cavities and strong focusing solenoids. Experiments have shown that there may be serious problems operating rf in the required magnetic fields. Experimental observations using vacuum rf cavities in magnetic fields are discussed, current published models of breakdown with and without magnetic fields are briefly summarized, and some of their predictions compared with observations. A new theory of magnetic field dependent breakdown is presented. It is proposed that electrons emitted by field emission on asperities on one side of a cavity are focused by the magnetic field to the other side where they induce mechanical fatigue leading to cavity surface damage in small spots. Metal is then electrostatically drawn from the molten spots, becomes vaporized and ionized by field emission from the remaining damage, and causes breakdown. The theory is fitted to existing 805 MHz data and predictions are made for performance at 201 MHz. The model predicts breakdown gradients significantly below those specified for either the International Scoping Study neutrino factory or a muon collider. Possible solutions to these problems are discussed, including designs for *magnetically insulated rf* in which the cavity walls are designed to be parallel to chosen magnetic field contour lines and consequently damage from field emission is expected to be suppressed. An experimental program that could study these problems and their possible solution is outlined. We also mention the use of high pressure gas as an alternative possible solution.

DOI: 10.1103/PhysRevSTAB.12.031002 PACS numbers: 29.20.−c, 29.27.−a, 52.59.−f

I. INTRODUCTION

Ionization cooling is the only practical method for cooling the muon beams in a neutrino factory [1] or a muon collider [2]. An ionization cooling channel is a tightly spaced lattice containing absorbers for reducing the momentum of the muon beam, rf cavities for restoring the axial momentum, and strong magnetic fields for focusing the beam at the absorbers. Efficient channels of this type have significant magnetic fields present over the normal-conducting rf cavities. Typical cooling channel frequencies range from 200–800 MHz, required gradients vary from 16 to 40 MV/m, and magnetic fields at the cavities can reach 5 T.

The front ends of neutrino factories and muon colliders also contain *phase rotation* channels that reduce the energy spread of the muon beam. These channels also have rf cavities located in a solenoidal focusing lattice, so that significant magnetic fields are present at the cavities.

Experimental data exists on the operation of 805 MHz vacuum rf in magnetic fields. These data were obtained with two very different cavity types: (1) a multicell cavity with open irises [3], and (2) a single ''pillbox'' cavity with irises closed with Cu plates or Be windows [4]. Both showed significant problems and will be discussed in this article.

There is very little data on operations of 201 MHz vacuum cavities in significant magnetic fields, although experiments are underway with local fields of about 1 T on a limited part of the cavity. Tests are planned for the 201 MHz cavity in fields of the order of 3 T and geometries that can be made close to those in the machine designs.

There is also data on the DC operation of a test cavity in high pressure hydrogen gas that showed no magnetic field dependence [5]. However, there may be other problems arising when an ionizing beam passes through such a gas filled cavity; in addition, such gas filled cavities cannot be used in the later stages of cooling for a muon collider because the Coulomb scattering in the gas would cause too much emittance growth.

A number of models have been proposed for rf breakdown without a magnetic field present. Many of the models assume field emission follows the Fowler-Nordheim relation [6] and that the local field is given by $\boldsymbol{E}_{\text{local}} = \langle\beta_{\text{FN}}\rangle \times \langle\boldsymbol{E}\rangle$, where $\langle\boldsymbol{E}\rangle$ is the macroscopic cavity field at the emission location and $\langle\beta_{\text{FN}}\rangle$ is an empirical constant. The value of β_{FN} is related to the presence on the cavity surface of microscopic *asperities*. These could include perturbances, cracks, grain boundaries, or other causes of local field enhancement. One or more of these mechanisms may also play some role in breakdown when a magnetic field is present. We now briefly give a description of some

models that do not explicitly depend on the external magnetic field.

A. Mechanical fracture model

The mechanical fracture model [7] assumes the following sequence of events: (1) The surface contains asperities at the top of which the local field is given by the average field multiplied by a Fowler-Nordheim field enhancement factor β_{FN}. (2) The outward electrostatic tension is equal in magnitude to the energy density of the field, hence it is proportional to the square of the field (7 GV/m would induce a tension of 300 MPa), breaks off the tip and the small piece now moves away from the remainder of the asperity. (3) The piece is bombarded by field emitted electrons from the remaining asperity and becomes vaporized and ionized. (4) Following this formation of a local plasma other mechanisms cause the plasma to spread or short out the cavity leading to breakdown. Within this model the breakdown occurs when the electrostatic outward tension at the asperity equals the tensile strength of the material.

B. Ohmic heating model

It has been suggested [8] that, when the field emission current density is sufficiently high, breakdown is initiated by Ohmic heating that melts the tip of an asperity. Once liquefied electrostatic forces would pull the molten material away, just as the broken piece of the asperity was pulled away in the first model. This molten material, as it lifts from the remains of the asperity, will be exposed to field emission from the remaining asperity left behind and it will be further heated, vaporized, and ionized to form a plasma. For submicron asperities, the time constant for achieving a steady thermal state is of the order of a nanosecond, so the temperatures reached depend only on the geometry, electrical resistivity, thermal conductivity, and current densities at the tip.

C. Thermal runaway model

This model [9] takes the temperature dependence of the resistivity and thermal conductivity into account. One can look at the relative rates of heating and cooling as a function of the effective temperature. For a low current density the cooling rises more rapidly than the heating and a stable temperature is possible. On the other hand, at higher current densities the rate of heating vs temperature rises faster than the cooling and the temperature will *runaway*. The actual critical temperature at the tip will be somewhat higher. It is worth noting that repeated heating to temperatures of this order may induce fatigue, leading to damage and an increased probability of breakdown after many rf pulses.

D. Reverse bombardment model

A fourth model [10] assumes that some initial mechanism generates a local plasma, a so-called *plasma spot*, that by itself does not directly cause breakdown. Plasma spots, tiny sources of light, have been observed in DC and pulsed gaps without breakdown. In this model, breakdown occurs when electrons emitted by the local plasma are returned to their source spots by the rf electric field. The energy given to the source by these returning electrons is required to cause the plasma to grow and cause the actual breakdown. But as we will see later in Fig. 7, at least for 805 and 201 MHz in the absence of an axial magnetic field, electrons emitted at the highest field location never come back to their source, no matter what their initial phase. This appears to be true for cavities in general, with the exception of emission on the axis in pillbox cavities. Yet breakdown on the axis of pillbox cavities is rarely observed.

E. Surface damage by heating

In our frequency range of interest, 200–800 MHz, the maximum surface field experimentally observed rises approximately as the square root of the rf frequency [11]. It should be noted that this dependency does not continue at frequencies above 3 GHz and measurements between 20–40 GHz show no frequency dependence [12]. Fatigue damage from cyclical surface heating appears to limit the gradients at higher frequencies. This damage is worse at locations with maximum surface currents, where surface electric fields are usually low. But the damage, which causes cracks to form at grain boundaries, can be so severe that breakdown is initiated in regions with both electric fields and surface current. Since this phenomena is only seen at such high frequencies, it is not expected to be a problem for neutrino factories or muon colliders.

Although the above discussion of breakdown without a magnetic field present suggests that Ohmic heating may initiate breakdown, this conclusion depends on a limited number of experiments; therefore one has to conclude that the initial mechanism that starts a breakdown is not fully understood yet. But there are some dependencies that appear fairly consistently: (i) Over a wide range of frequencies (0.2 to 3 GHz), breakdown gradients are approximately proportional to the square root of the rf frequency, and this dependency arises because of changes in the observed field enhancement factor β_{FN}. (ii) Breakdown appears dependent on the required energy to melt a given volume of the electrode material. In vacuum waveguide experiments [13] this dependence is again caused by changes in β_{FN}, rather than in the local fields. (iii) Breakdown occurs at lower gradients for long rf pulses than for short pulses, and there is some indication that this too arises from the pulse lengths influence on β_{FN}.

A reasonable assumption is that, whatever the initial cause, the effect of a breakdown is to remove asperities and consequently to lower β_{FN}. At the same time, however, the breakdowns, depending on the energy available, will create new asperities, thus increasing β_{FN}. In a *conditioned* cavity, these competing processes reach an equilibrium.

Fewer models have been developed that take the magnetic field dependence of breakdown explicitly into account. In the "twist" model [3], the magnetic dependence arises from the torque introduced at asperities. In this paper we introduce a new model of magnetic field dependent breakdown. It is proposed that electrons emitted by field emission on asperities on one side of a cavity are focused by the magnetic field to the other side where they cause fatigue in the cavity surface in small spots. Metal is then electrostatically drawn from the surface, becomes vaporized and ionized by field emission from the remaining damage, and causes breakdown. The model is quantitatively described in Sec. III and predictions are made for rf cavity performance at 201 MHz.

II. RECENT EVIDENCE FOR RF BREAKDOWN IN MAGNETIC FIELDS

An active program of R&D on normal-conducting rf cavities is taking place at the Mucool Test Area (MTA) at Fermilab [14,15], as part of a national program of neutrino factory and muon collider development. The MTA group is studying the dependence of 201 and 805 MHz cavity performance on magnetic fields as well as materials, gas pressure, and coatings.

In all cases discussed here, the cavities or waveguides were "conditioned" prior to achieving the quoted gradients [3,16]. After one or more breakdowns at one gradient, the cavity subsequently withstood a somewhat higher gradient. Conditioning started by slowly ramping up the rf input power. With a constant power level the cavity was allowed to outgas. During the conditioning multipactoring, sparking, dark current (with x rays), and vacuum fluctuations were monitored [3]. The breakdown gradient was loosely defined to be the limiting gradient above which sparking cannot be eliminated with further conditioning. The sparking rate was $\approx 1/3000$ pulses at the breakdown gradient [16]. Typically, many hundred successive breakdowns were induced prior to the cavity reaching its "final gradient." The cavity runs stably when the input gradient is slightly below that threshold. The final breakdown limits were fairly reproducible. Studies of the pulse length dependence of the breakdown have not been done.

Four cavities were used to measure the effect of magnetic field on the maximum gradient. The first one was a six-cell open iris 805 MHz cavity (Fig. 1. The second was a 805 MHz pillbox (Fig. 3) with replaceable windows (Cu, Be) which was later modified to accommodate "buttons" to enhance the electric field at the surface. The third one was a 201 MHz pillbox with Be windows. The fourth one was a high pressure gas test cavity (Fig. 4). Some important properties of these cavities are shown in Table I. Only one example of each type of cavity has been constructed so far.

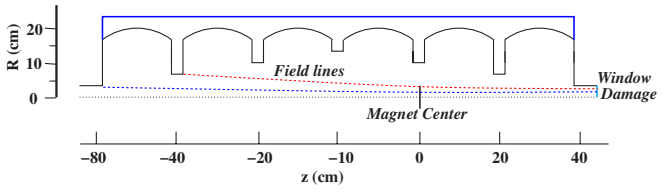

FIG. 1. (Color) Schematic of the multicell cavity first tested in the "Lab-G" magnet at Fermilab. The lines shown are the magnetic field lines extending from two irises to the end window.

TABLE I. Standard parameters of the tested cavities.

Six-cell open iris 805 MHz	
Length (cm)	16.2
Z_s (MΩ/m)	31
Q_o	32 813
Power (MW/m) for 30 MV/m	29
Repetition rate (Hz)	15
Pillbox 805 MHz	
Length (cm)	8.1
Radius (cm)	15.62
Be window diameter (cm)	16
Be window thickness (μm)	127
Z_o (MΩ)	38
Q_o	18 800
Gradient (MV/m)	30
Pillbox 201 MHz	
Length (cm)	43
Radius (cm)	61
Be window diameter (cm)	42
Be window thickness (μm)	380
Z_s (MΩ/m)	22
Q_o	53 000

A. Experimental operations of a multicell 805 MHz open cavity in approximately axial magnetic fields

A multicell open rf cavity (Fig. 1) was built at the MTA as an example of the type of cavity needed in an ionization cooling lattice. Such lattices used early in a cooling channel would use 201 MHz, but higher frequency and high magnetic fields would be needed for later cooling. The six-cell cavity was designed with iris apertures tailored to fit the beam profile in the matching fields [3] of the cooling lattice. The cavity was tested with and without magnetic fields. The available fields could not match the lattice design, and the cavity could not be positioned symmetrically in the magnet, so the fields used in the test were asymmetrical. The maximum achieved surface gradients were quite high (≈ 53 MV/m), comparable with those in the gas filled cavity, and were not strongly dependent on the magnetic fields (Fig. 2). However, both x rays and dark currents were greatly increased with the magnetic field on. After some time, vacuum was lost, and it was found that the end vacuum window was so damaged as to cause the vacuum leak.

It was found that the location of the window damage corresponded to a focused dark current coming from one of

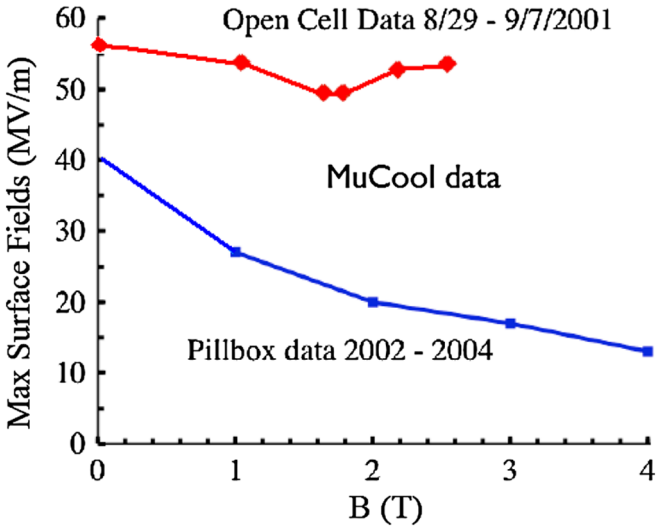

FIG. 2. (Color) Maximum surface field vs axial magnetic field in 805 MHz cavities (data from Refs. [29,30]).

the high field irises. In addition, radiation damage patterns were observed showing that many beamlets were focused by the magnetic fields onto the end window. There was no indication that dark currents from one high gradient iris were focused onto another, which may explain why the maximum achieved gradients remained high.

B. Pillbox cavity breakdown in magnetic fields

In a linac with open irises, the peak surface fields are typically a factor of 2 higher than the average accelerating gradient. After designing the multicell open iris cavity, it was realized that with muons one could introduce thin Be windows at each iris and obtain accelerating gradients much closer to the maximum surface fields. In addition, the resulting pillbox cavities give more acceleration for a given rf power. A test pillbox cavity was thus designed (Fig. 3) and tested in a magnetic field. This time the cavity was mounted in the center of the magnet and could thus be tested with symmetrical fields. It was also tested with one of the magnets coils unpowered to give asymmetrical fields and with the coils powered in opposite directions to study the effects with these different field geometries.

Without field the maximum achieved gradients [4] were somewhat lower than for the multicell cavity, but this was, at least to some extent, the result of more conservative operation after the severe damage seen in the earlier cavity. With magnetic fields, the maximum gradients were found to be strongly dependent on field (Fig. 2). It was also found that over time its performance deteriorated. Examination of the inside of the cavity showed severe pitting on the irises. The Be windows themselves showed no visible damage, but there was a spray of Cu over their surface and Cu powder in the bottom [17].

More data [18] has been taken since the cavity had suffered significant damage. These data (not shown) lie

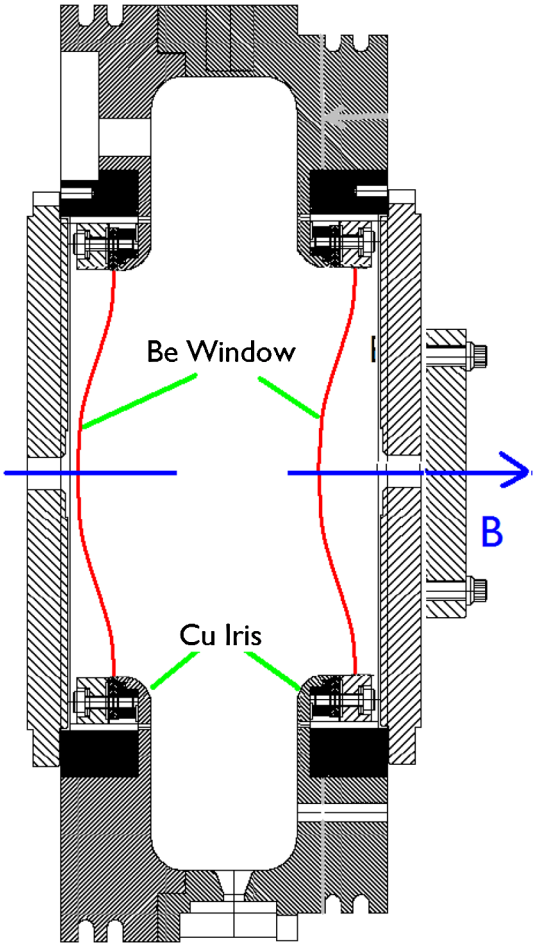

FIG. 3. (Color) 805 MHz pillbox cavity with curved Be windows.

at somewhat lower breakdown gradients and presumably correspond to a now higher value of the Fowler-Nordheim β_{FN}.

The pillbox cavity has more recently been tested [19] with one of its two Be windows replaced by a flat Cu plate with an easily replaceable central "button." The button had dimensions such that the local field on the tip was 1.7 times that on the outer Cu "iris." The intent was to allow a study of magnetic field dependent breakdown as a function of materials, the assumption being that breakdown would occur at the high gradient on the tip of the button. The cavity was found to operate with gradients on the button significantly higher (by approximately a factor of 1.7) than had been observed without the button. It was noted, however, that this breakdown occurred with gradients on the iris, and on the flat support plate, that were essentially the same as those present without the button. This suggested that breakdown was not occurring on the button, but rather at other locations that did not have the 1.7 times field enhancement: on the irises and/or the flat button support plate. When the cavity was later disassembled it was indeed found that there was little damage on the button,

where the field was maximum. But there was significant damage in a distinct band from 3 to 6 cm on the TiN coated Cu support plate [see Fig. 11(a)]. Using a TiN coating helped suppress multipactoring.

C. 805 MHz high pressure gas filled test cavity experiments

A simple test cavity (Fig. 4) has been operated with hydrogen at different pressures and with buttons made of different materials that define the small high gradient gap [5]. It was found that, at lower pressures, the breakdown gradient follows the Paschen prediction, but at higher pressures the gradient is limited to values (50 MV/m for Cu) close to those observed (53 MV/m) in an open multicell vacuum cavity after conditioning. This similarity in the observed maximum gradients suggests that the initiating mechanism for breakdown in the high pressure gas and vacuum cavities is the same. No change in breakdown was observed in the presence of an external magnetic field of 3 T. This is as would be expected from our new model for vacuum breakdown with magnetic fields that is described in Sec. III.

Tollestrup [20] has studied the likely effects of a muon beam passing through gas filled rf cavities. His analysis suggests that the lifetime of the electrons and ions produced by the ionization of those beams are long compared with the likely duration of the muon beams. It is further concluded that such electrons in the cavity will be driven backwards and forwards as the rf voltage oscillates, and that this will lead to heating of the gas and loss of the rf energy. The introduction of other gases to rapidly capture the electrons may avoid this problem, but there remain concerns that the presence of accumulating numbers of ions will cause trouble.

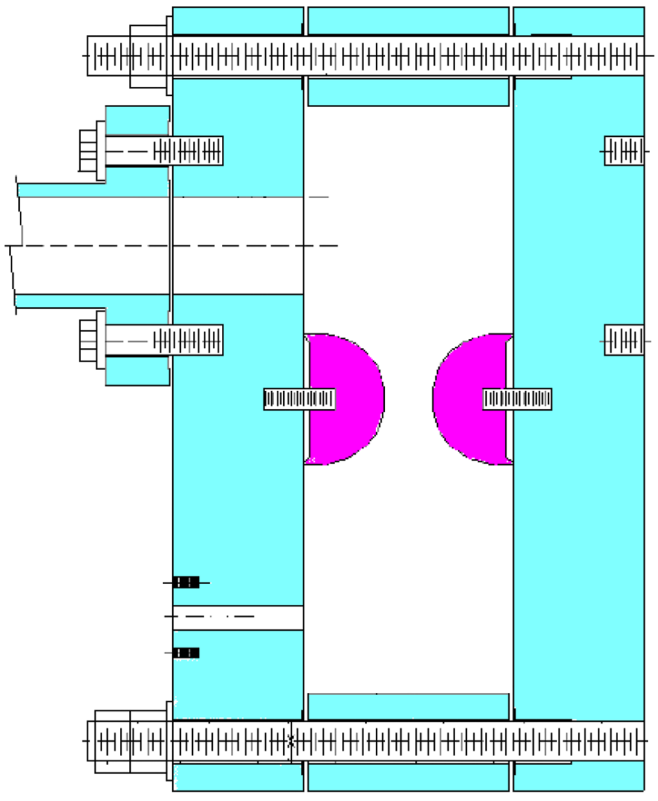

FIG. 4. (Color) Schematic of the test cavity with replaceable buttons (half-spherical surfaces at the center) defining the high gradient gap.

In any case, it must be noted that high pressure gas cannot be used in the later cooling stages of a muon collider where the emittance is very small. In these cases the Courant-Snyder $\beta_\perp$ must be very small where any material is introduced. This can be achieved in local areas, or inside very high field solenoids, but not over the lengthy rf systems. Final cooling for a muon collider will thus inevitably require vacuum acceleration near strong fields.

D. Dark currents

The dark current spectrum could be measured directly using absorber range and a beam transformer [3]. The maximum dark current energy was measured with a magnetic spectrometer [3]. The x rays produced in association with the dark current could be measured with radiation monitors. Increases in cavity vacuum could be measured with a residual gas analyzer. When dark current distributions are studied as the gradient is increased by this conditioning, it is again found [17] that it is the enhancement β_{FN} that is decreasing and not that the local field is increasing.

III. BREAKDOWN MODELS WITH EXTERNAL MAGNETIC FIELDS

In this section we will first discuss a previously published model of breakdown in magnetic fields. Then we will describe our new model in detail and compare the predictions of the models with recent experiments.

A. Published breakdown model with magnetic fields

It has been proposed in the twist model [3] that the magnetic field dependence on breakdown arises from the torque forces on an asperity. These forces are due to the inflow of current that feeds the field emission reacting to the external magnetic field; that is $F \propto I \times B$, where $\boldsymbol{E}$ is the cavity electric field gradient and approximately $I \propto \boldsymbol{E}^{10}$ [3]. Thus for breakdown at a fixed force F, we expect

$$\boldsymbol{E}_{\mathrm{breakdown}} \propto B^{-1/10}. \tag{1}$$

In Fig. 5 the observed pillbox cavity breakdowns are plotted as a function of the external average magnetic field. The points plotted are those where both superconducting coils were powered so that the magnetic fields were relatively uniform over the cavity. The dependency predicted by this mechanism is shown by the solid black line; it is a

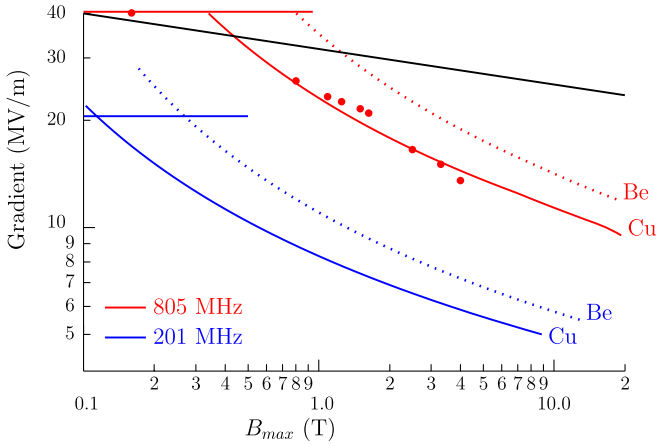

FIG. 5. (Color) Breakdown gradients vs axial magnetic fields. Black line is dependency predicted by asperity twist model. Red lines are fit to the plotted Lab-G [4] breakdown data. Blue lines are the calculated values for a 201 MHz cavity. Dotted lines are for Be surfaces.

poor fit at higher fields where the breakdown gradient falls much faster than predicted.

B. Introduction to the proposed mechanism

We propose a new model for breakdown with a magnetic field that is independent of the breakdown mechanism in the absence of magnetic fields (see Fig. 6). Breakdown occurs by this mechanism *only* if its breakdown gradient is lower than that from the case without a magnetic field. Its elements are: (i) "dark current" electrons are field emitted from an asperity, accelerated by the rf fields, and impact another location in the cavity. In the absence of a magnetic field these impacts, depending on their phase of emission, are spread over large areas and do no harm. (ii) With sufficient magnetic field the emitted electrons are focused to small spots, where they heat the surface sufficiently to cause damage. The mechanism of damage could be melting, but is more likely to arise, at lower temperatures, from fatigue induced in the material by the repeated local energy deposition. (iii) If the location of such damage is at a low gradient location there is no immediate breakdown, but the damage could accumulate until, for instance, a hole is made in a window. (iv) If the electrons are focused onto a location with high surface rf gradient, then the local damage will provide new asperities with higher Fowler-Nordheim β_{FN}, thus initiating the breakdown.

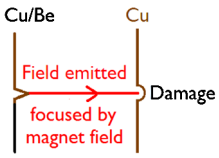

FIG. 6. (Color) Proposed mechanism for breakdown with an external magnetic field.

Breakdown will be dependent on (a) the Fowler-Nordheim field enhancement β_{FN} that determines the strength of the field emitted current, (b) the local geometry of the asperity that will determine the initial particle distributions and effects of space charge, and (c) on the geometry and magnetic fields that focus the electrons onto other locations.

C. Electron motion in a cavity

A program CAVEL [21] tracks particles from arbitrary positions on the walls of a cavity until they end on some other surface. The program uses SUPERFISH [22] to determine the rf electric and magnetic fields, and uses a map of external magnetic fields calculated for arbitrary coil dimensions and currents. Figure 7 shows trajectories, for differing initial rf phases, starting from the highest field location on an iris. Without an external magnetic field, none of the trajectories from the high field location come back to their common origin. Tracks emitted at a phase of 20° do hit the opposing iris at a high gradient location, but they are not focused there and are spread out over a significant distance. However, when a sufficient external axial magnetic field is present, the tracks are either focused to the high gradient location on the opposite iris or returned to their source.

There remains a small dependency of the arrival positions with phase, which arises from the combined effects of the perpendicular external and rf magnetic fields, but this dependency is small. If there were no other mechanism to spread out the electrons, then damage would appear as lines, which are not observed. In addition, damage would be much worse on the axis than at larger radii, also not observed. From this, one can assume that the damaging

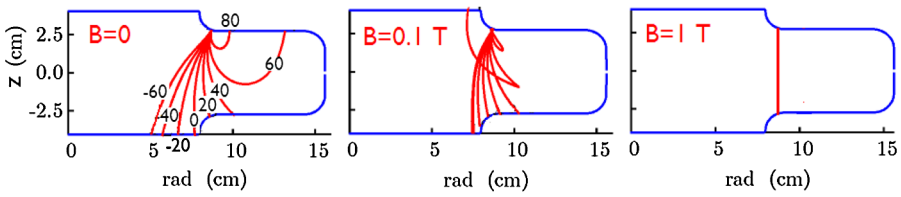

FIG. 7. (Color) Trajectories of electrons field emitted at different phases from the highest surface field location in an 805 MHz pillbox cavity with no external magnetic field (left), an axial field of 0.1 T (center), and an axial field of 1 T (right). The axial electric field is 25 MV/m. Phases are in degrees relative to the maximum.

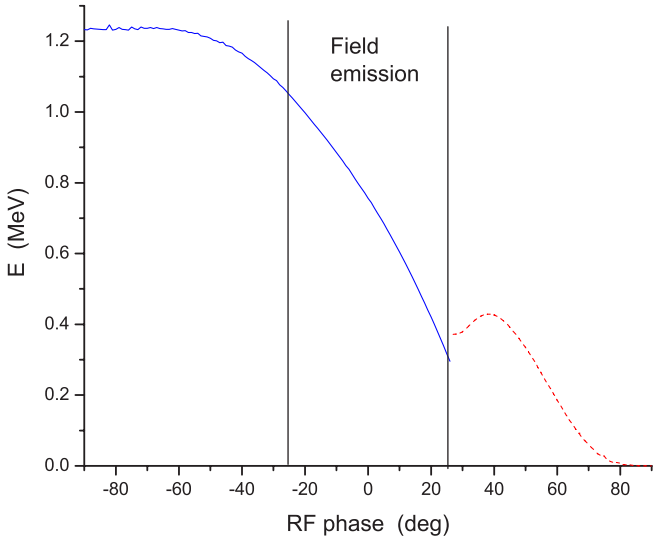

FIG. 8. (Color) Energies of electrons on impact vs their phase of emission. Red indicates electrons that returned, blue those that arrive on the next iris. Axial gradient is 25 MV/m.

emission is dominated by field emission which is restricted to a limited range of phases ($\pm \approx 20°$) and that another mechanism, such as space charge, spreads the beamlets out to a greater extent than this phase dependent effect. Figure 8 shows the energies of the electrons on impact and indicates which phases are returned and which arrive on the next iris. Field emitted electrons ($\pm 25°$) do not come back, but are focused to a local area on the opposite iris. Experimental observations [3] of the time structure of dark current show that this dark current is concentrated at phases close to zero. It seems unlikely then that, even with an external axial magnetic field, significant currents of electrons will be returned to their source.

The electron energies for the 805 MHz cavity with axial rf fields of 25 MV/m are approximately 1 MeV. For a 201 MHz cavity, and the same gradient, they are of the order of 4 MeV. At these energies, the electrons penetrate to significant depths in the Cu cavity walls. If Be is used, the penetration is even deeper. The relative surface heating and thus probability of fatigue and damage depends on the fraction of energy deposited in a surface layer, taking into account thermal conduction away from the deposition. A full calculation would include the time dependence of both deposition and conduction. As an approximation, the temperature rise is estimated from the deposition in a depth corresponding to the thermal diffusion depth at the surface.

D. Field emitted electron current

It is assumed in all models that breakdown is initiated at asperities, where the local electric fields is higher, by a factor β_{FN} introduced by Fowler-Nordheim [6]. The average values of these factors can be determined by observing the electron currents (dark current) emitted by the sum of many asperities, each of which has a specific value of β_{FN}. The field emitted average electron current density $J_F(\frac{\mathrm{A}}{\mathrm{m}^2})$ for a surface field $\boldsymbol{E}(\frac{\mathrm{V}}{\mathrm{m}})$, and local field $\boldsymbol{E}_{\mathrm{local}} = \beta_{\mathrm{FN}}\boldsymbol{E}$ is given by [8]

$$J_F = 6 \times 10^{-12} \times 10^{4.52\phi^{-0.5}} \frac{\boldsymbol{E}_{\mathrm{local}}^{2.5}}{\phi^{1.75}} \exp\left[-\frac{\zeta\phi^{1.5}}{\boldsymbol{E}_{\mathrm{local}}}\right], \quad (2)$$

where ϕ is the material work function in (eV) ($\phi = 4.5$ eV for Cu) and

$$\zeta = 6.53 \times 10^9 \ (\mathrm{eV})^{-1.5} \left(\frac{\mathrm{V}}{\mathrm{m}}\right). \quad (3)$$

In vacuum cavities with a thin window, one can measure some fraction of all field emitted electrons and observe its field dependence. From this dependence, given an assumed work function ϕ, one can then extract an average value of $\langle\beta_{\mathrm{FN}}\rangle\langle\boldsymbol{E}\rangle$.

It is reasonable to assume that breakdown occurs where the local field and thus $\beta_{\mathrm{FN}}\boldsymbol{E}$ is maximum, and thus higher by a factor α than the average value determined from the gradient dependence of the dark current from many asperities, so

$$\frac{\boldsymbol{E}_{\mathrm{local}}}{\alpha} = \langle\beta_{\mathrm{FN}}\rangle\langle\boldsymbol{E}\rangle, \quad (4)$$

where $\alpha \gtrsim 1$ depends on the probability distribution of β_{FN}.

Observed breakdown gradients are found to depend on frequency [23], rf pulse length, and cavity dimensions, but it has been found [17] that, over a range of frequencies from DC to a few GHz, and for differing pulse lengths, cavity dimensions and also in waveguides, the values of $\frac{\boldsymbol{E}_{\mathrm{local}}}{\alpha}$ fall in a relatively narrow range around 7 GV/m. Breakdown thus appears to be related to the local electric fields at asperities, or to the field emitted currents that are strongly dependent on these fields.

The field emission current density is approximately proportional to the local field $\boldsymbol{E}_{\mathrm{local}}$ to the tenth power [3].

E. The effects of space charge on the transverse distribution of field emitted current

Without an asperity and emission from a small area, the space charge forces give transverse momenta to emitted electrons causing the beamlet's radius to increase. As the beamlet increases in radius and the electrons are accelerated, the space charge forces drop and it can be shown that the induced *rms* transverse momentum is $\sigma_{p\perp} \propto \sqrt{I}$. But if the electrons are emitted from the tip of an asperity then they will first be spread by the approximately spherically symmetric local electric fields, and the effect of the space charge is consequently modified.

A simple simulation was performed (see Fig. 9). The initial electric fields were assumed to have strength $\beta_{\mathrm{FN}}\boldsymbol{E}$, and exact spherical symmetry out to a distance X. Beyond

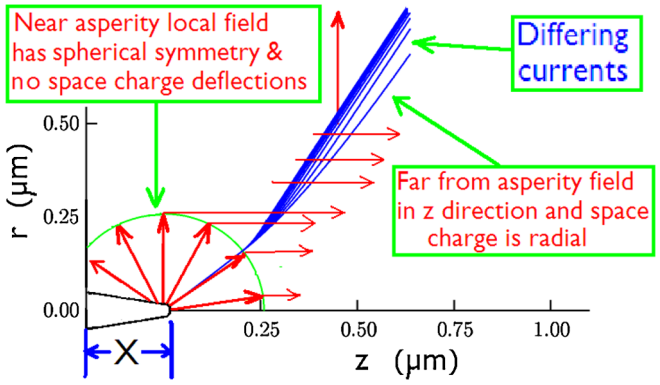

FIG. 9. (Color) Schematic of approximate simulation of space charge effects on electrons emitted by an asperity.

this distance, the fields were assumed to be perpendicular to the average surface with strength $\boldsymbol{E}$. No space charge effects are included in the spherically symmetric part. Radial space charge forces, inversely proportional to an average radius, are assumed beyond the distance X. We found that with $X = 0.2$ μm, the transverse momenta could be approximated by $\sigma_{p\perp} \propto I^j$, but with the power $j \approx 0.3$ instead of 0.5 as in the simple case without asperity. Since neither the asperity height nor its shape are known, it is reasonable to treat the exponent j as an unknown that is fitted to the experimental data. In a better simulation, this fit would give us information on the asperity dimensions, but this model is too simple for this at this stage. At distances from the source large compared with X, space charge becomes negligible, but the transverse momentum is focused by the axial magnetic field, giving a beamlet with an rms radial size $\sigma_r \propto \frac{I^j}{B}$, where B is the axial magnetic field. The power per unit area W of the electron beamlet hitting the opposing surface is given by

$$W = \frac{I\mathcal{E}_e}{\pi\sigma_r^2} \propto \frac{I^{(1-2j)}\mathcal{E}_e B^2}{\pi}, \tag{5}$$

where $\mathcal{E}_e$ is the final electron energy in eV determined from CAVEL [21] simulations. $\mathcal{E}_e$ is plotted in Fig. 10 as a function of the axial rf gradient, for (1) 805 MHz pillbox cavity [4], and (2) 201 MHz cavity designed for the MICE cooling experiment [24].

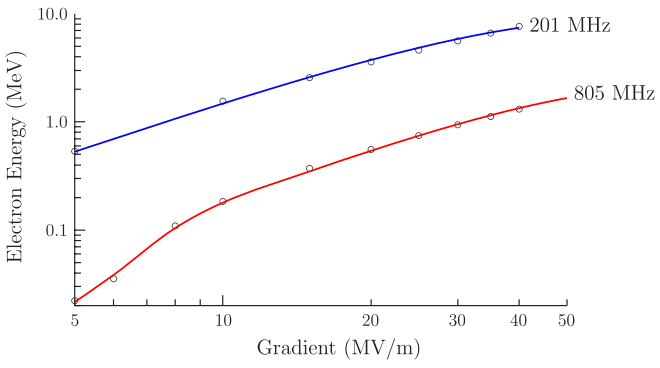

FIG. 10. (Color) The simulated final electron energy $\mathcal{E}_e$ as a function of axial rf gradient for (red) a 805 MHz pillbox cavity, and (blue) a 201 MHz cavity.

F. Fraction of energy deposited in the thermal diffusion depth

The thermal diffusion length δ corresponding to the rf field pulse duration $\tau(s)$ is $\delta = 10^{-2}\sqrt{D\tau}$, where $D = \frac{K}{\rho C_s}$ is the thermal diffusion constant in (m), K is the thermal conductivity, and C_s the specific heat. It is assumed that all the energy deposited in this diffusion depth is spread uniformly within that depth δ. The penetration depth d in (μm) of low energy electrons is approximately given by [25]

$$d = 0.0267\frac{A}{\rho Z^{0.89}}\mathcal{E}_e^{1.67}, \tag{6}$$

where $\mathcal{E}_e$ is the electron incident energy in (keV), ρ is the material density in ($\frac{\text{g}}{\text{cm}^3}$), and Z and A are the atomic number and atomic weight, respectively.

If $\mathcal{E}(x)$ is the energy of an electron with penetration depth x and we define Q as the fraction of the electron energy deposited in the thermal diffusion length δ, then (i) For electrons whose penetration depth is less than the diffusion depth ($d < \delta$): $Q = 1$. (ii) For electrons whose penetration depth is greater than the diffusion depth, but not much greater ($\delta < d < 10 \times \delta$) then $Q = \frac{\mathcal{E}_e - \mathcal{E}_e(d-\delta)}{\mathcal{E}_e}$.) iii) For electrons with penetration depth $d > 10 \times \delta$ then $Q = \frac{\frac{d\mathcal{E}_e}{dx}\delta}{\mathcal{E}_e}$.

G. Dependency of local temperature rise

The surface temperature rises as a fraction of the material melting temperature T_m is given by

$$\frac{\Delta T}{T_d} \propto W\left(\frac{\tau Q}{\delta\rho C_s T_d}\right), \tag{7}$$

where ρ is the density, C_s is the specific heat, τ is the rf pulse length, taken to be 20 and 160 μs at 805 and 201 MHz, respectively ($\tau \propto \lambda^{3/2}$), and T_d is the temperature that, when cycled, causes damage. We will assume that $T_d \propto T_m$. Parameters used for Cu and Be are given in Table II.

H. Fit to field dependence data from *Lab-G* pillbox and predictions for 201 MHz

The above is a very approximate analysis. A full simulation of the problem is being pursued. The simulations were done with uniform magnetic field; tracks were only simulated from the single maximum gradient location; electron impacts were assumed at 90° to the surface; the thermal diffusion calculation ignored the rise time shape and used an approximate calculation; both current scale

TABLE II. Atomic and nuclear properties of Cu and Be.

	Z	A	K (W/cm-°C)	ρ (g/cm^3)	C_s (J/g-°C)	D (cm^2/s)	$\delta(805)$ (μm)	$\delta(201)$ (μm)	T_m (°C)
Cu	29	63.5	4.01	8.96	0.385	1.16	48	186	1085
Be	4	9.0	2.18	1.85	1.825	0.81	40	155	1287

and space charge strength were normalized to fit data and a proportionality between damaging and melting temperatures was assumed. However, if this simple approach can qualitatively fit the data, it should allow a qualitative extrapolation to 201 MHz and other materials. A fuller simulation should provide more quantitative results. The red curved line in Fig. 5 shows the fit to the 805 MHz Cu cavity in Lab-G breakdown data [4]; the fitted value of the current exponent was $j = 0.35$. The black line in the plot shows the dependence predicted by the twist model [3], which does not fit the data well. The dashed lines show the calculated breakdown limits for Be. The horizontal red line indicates the gradient limit from the assumed model without magnetic fields, assuming the local field limit to be 7 GV/m.

I. Extrapolation to 201 MHz

Let us recall that, without an external magnetic field, breakdown gradients follow approximately a $\sqrt{f}$ behavior. Under the assumptions used here [7], the local field at breakdown is independent of the frequency; this implies that β_{FN} decreases approximately as $\frac{1}{\sqrt{f}}$. Using this assumption, and using the appropriately modified diffusion depth, the predicted breakdown limits at 201 MHz, for Cu (solid blue line) and Be (dashed blue line), are shown in Fig. 5. The predicted 201 MHz breakdown gradients are seen to be a factor of 2 to 2.5 below those for 805 MHz. This factor comes primarily from the higher expected β_{FN}, but also from the longer rf pulse duration and thus longer time to heat and damage the surfaces. The higher required gradients specified for neutrino factory phase rotation and cooling (15 MV/m at $B \leq 3$ T) are well above this predicted level.

J. Other experimental results consistent with this analysis

The observed damage on the button support plate in the pillbox cavity discussed in Sec. II B is shown in Fig. 11(a). These observations are consistent with the breakdown mechanism described in this paper. SUPERFISH [22] calculations showed that the fields on the Be window opposite the button and support plate were maximal just in the band 3 to 6 cm, where the damage was observed [see Fig. 11(b)]. In this model, emission from the Cu button, falling on the Be is less liable to cause damage and breakdown, whereas the emission from the Be focused onto the Cu plate should cause damage just where the gradients were maximal on the Be.

IV. POSSIBLE SOLUTIONS, OR REDUCTIONS, OF THESE PROBLEMS

There are several possible approaches to overcoming these breakdown problems in a muon collider or neutrino factory. (i) Redesign the phase rotation and cooling channels to use lower rf fields. This approach would clearly hurt performance, and, in addition, risks a slow deterioration of

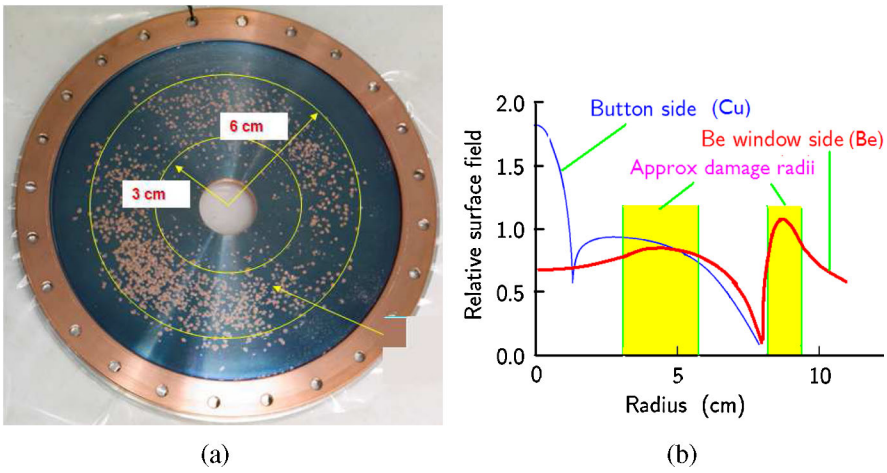

(a) (b)

FIG. 11. (Color) (a) Button support plate showing damage band between 3 and 6 cm radius. (b) Surface fields on Be (red) and Cu (blue) vs radius, with bands showing where damage was concentrated (data from Ref. [19]).

performance as occasional breakdown events continue to spray Cu around the cavity—as observed in the pillbox tests. (ii) Use cooling lattices with high pressure hydrogen gas in the rf cavities. No degradation of rf performance has been observed in the small 805 MHz test cavity with axial magnetic fields and rf gradients similar to those in vacuum cavities. If the loading from beam induced electrons is not a problem, or is slowed by introducing gas impurities, then this solution should offer no loss of performance in the early cooling stages. But to cool to very low emittances, it will probably require lattices with lower Courant-Snyder β at the absorber than can be achieved in the rf. In this case, the addition of hydrogen gas at the higher βs in the rf would cause unacceptable emittance growth. So for later cooling, high pressure hydrogen gas is probably not a solution. (iii) Build cavities with exceptionally good surfaces so that the β_{FN} is sufficiently low initially that no breakdown occurs. With atomic layer deposition (ALD) this may be a realistic option [26]. The fear would be that a single breakdown spoils the surface in such a way that there will be a cause of further breakdown and a conditioning that approaches the same gradient limits seen in a conventional cavity. (iv) Construct cavities of materials that would be more resistant to damage from the impact of the focused dark current beams. The lack of observed damage on the Be windows suggests that if a cavity could be constructed of Be little damage would be observed. (v) Design lattices with magnetic field shielded from the rf. The above prediction suggests that, so long as the field is less than about 0.2 T, no adverse effects will be observed. Attempts to design such lattices have, unfortunately, shown significantly worse performance. (vi) Design lattices using multicell open cavities, with alternating current coils in their irises (Fig. 12). In this case, as in the original multicell

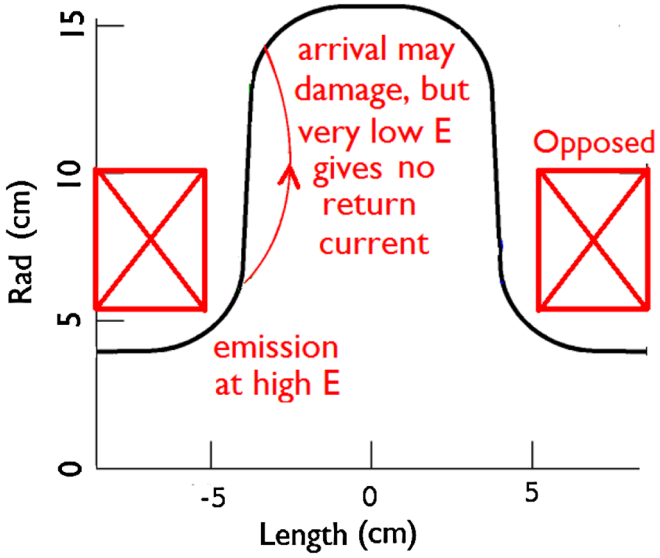

FIG. 12. (Color) Open cavity with alternated solenoid coils in irises.

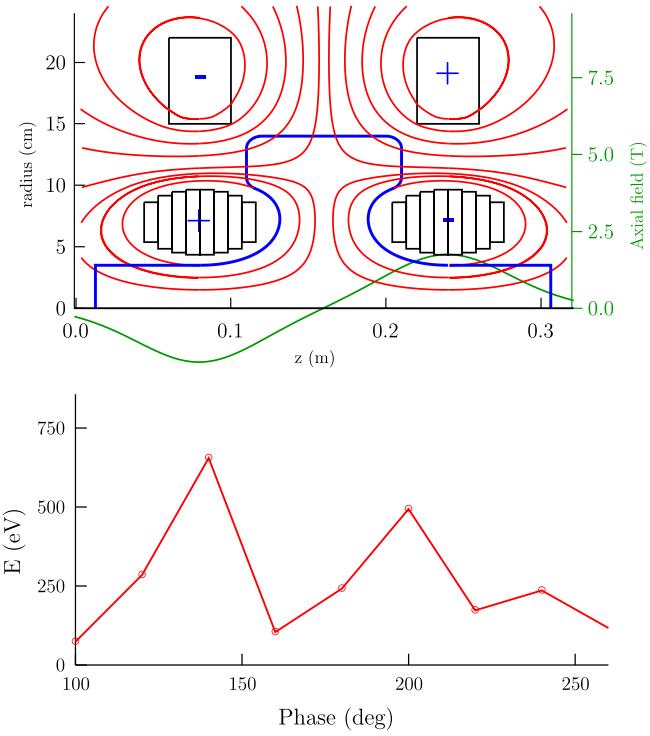

FIG. 13. (Color) Top: Magnetic field lines from coils in a cavity lattice, together with cavity shape that follows these field lines. Bottom: Energies of returning electrons as a function of their initial phase.

open cavity tests, the focused electrons would be directed to low field regions in the cavity and would thus not initiate breakdowns. Nevertheless damage done to those locations and molten Cu ejected from such damage could cause eventual deterioration of performance. In addition, the use of open, instead of pillbox, cavities implies lower acceleration for a given surface field. (vii) Damage might be eliminated if cavities were designed such that all high electric gradient surfaces were parallel to the magnetic fields (Fig. 13). This could provide "magnetic insulation" [27]. Dark current electrons would be constrained to move within short distances of the surfaces, would gain little energy, would cause no x rays, and do no damage. Possible difficulties might be: (a) cavities so designed will not give optimum acceleration for given surface fields, and (b) multipactoring might occur, now that the energies with which electrons do return to the surfaces are in the few hundred eV range where secondary emission is maximal.

V. EXPERIMENTS NEEDED TO STUDY THESE PROBLEMS

It is critically important to the development of a future neutrino factory or muon collider that a practical solution be demonstrated for the problem of rf breakdown in magnetic fields. This will require a well thought-out program

that begins with simple experiments and leads eventually to tests of an actual part of a cooling lattice. Three important experiments are already planned for the MTA.

(1) The testing of the existing 201 MHz cavity in magnetic fields similar to those in current MICE and cooling designs. This experiment is currently being carried out and some preliminary data at low field is known, however we do not include them as the results have not being published yet.

(2) Operating a high pressure hydrogen filled test cavity in a proton beam to study the possible breakdown and rf losses due to the ionization of the gas by the beam.

(3) Experiments with a simple vacuum pillbox cavity. The pillbox cavities that have so far been tested have relatively complex shapes, and the simulations of their performance with fields in differing directions are complex. It is thus desirable to test a simple pillbox shaped cavity whose performance would be easier to simulate. Two square cavities [28] (Fig. 14) have been designed so that it can be mounted in the center of the Lab-G magnet in at least two orientations: with its axis parallel to that of the solenoids or perpendicular to it. Ideally it should be possible to test it at other angles as well. Such a simple cavity design is also a good test vehicle for testing surface treatments including atomic layer deposition. Since the design is so simple, several versions could be made to compare their performances.

As illustrated in Fig. 15, CAVEL simulations of a cavity with its axis perpendicular to the solenoid axis show that the electrons are constrained to lie within a very small distance from the surface and gain little energy. Such a cavity would test whether multipactoring is a serious problem. In addition, if such a cavity were tested with the emission surface at a small angle to the field, then the electrons could gain some energy, but would end up on the cylindrical outer surfaces where there would be no electric field. This would test the configuration of the coil-in-iris solution without the shape modified to achieve magnetic insulation. Surface damage might be expected, but it should not cause breakdown.

Whatever the results of these tests, further experiments will likely be needed to study the observed problems at 805 MHz and test possible solutions. If the tests of the

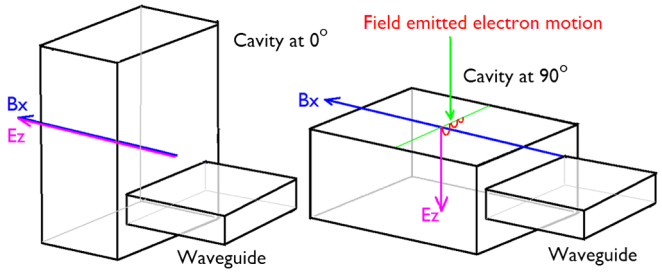

FIG. 14. (Color) Simple pillbox cavity with mounting in two orientations within the Lab-G solenoid.

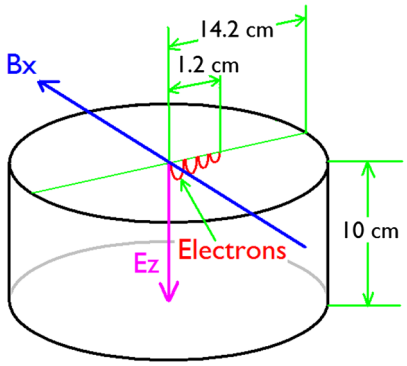

FIG. 15. (Color) A schematic illustration of an emitted electron's orbit when the magnetic field is parallel with the emitting surface.

201 MHz cavity in magnetic fields show problems also at that frequency, then further 805 MHz tests would be needed to explore solutions for these lower frequencies. Eventually, however, tests of any proposed solutions would have to be done at 201 MHz.

If with the proton beam the rf losses in the 805 MHz test cavity are sufficiently low, then further tests of high pressure gas filled cavities will be needed. In particular, cavities must be tested with more stored energy and with a similar shape to those needed. Thin windows must be designed, safety problems must be addressed, and beams with time structure and intensity nearer to those in the applications should be employed.

A number of other possible experiments have been considered to demonstrate a practical solution to the breakdown problem. These could be fairly simple at the beginning, but could evolve into a test stand capable of investigating many possible solutions.

A. A single cell experiment with magnetic insulation

In this experiment (Fig. 16) superconducting coils would be mounted on either side of a cavity whose shape is such that the magnetic fields are strictly parallel with the high gradient surfaces. The two coils close to the open pipe are powered in opposite directions. A second pair of coils is mounted outside the inner coils and powered with currents in the opposite direction to the inner coils. The coils would be separately powered so that the sensitivity to deviations from the insulated condition can be studied.

The rf cavity would be operated at liquid nitrogen temperatures in order to minimize the radiation falling on the superconducting coils that will be very close to its surfaces. There would be a vacuum both outside the rf cavity (for thermal insulation) and inside the cavity, although the quality of the latter should be higher, and would be separately monitored. Superinsulation and an outer liquid nitrogen shield are needed but not shown. Tuning of the cavity would be provided by axially squeezing or stretching the cavity. A variant of this experiment would have Be win-

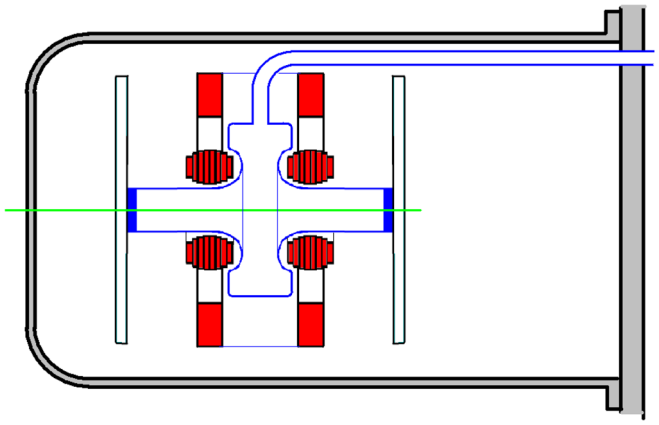

FIG. 16. (Color) Schematic of a single cell with magnetic insulation. The colored areas represent the cross section of superconducting solenoids; the central outline is the rf cavity whose body follows the surface of constant magnetic field.

dows, making it into more of a pillbox design and raising the accelerating field. This would not provide such complete magnetic insulation but, because of the special properties of the Be, it might still have acceptable performance.

B. A multipurpose test stand for these experiments

It is proposed that this and the following experiments would be carried out on a multiexperiment test stand. To allow ease of assembly, mounting of instrumentation, and making changes, all connections (rf, cryogens, magnet, and instrumentation leads, etc.) would be brought in through a single support plate (on the right side in the illustration). The vacuum container would be in the form of a dome that joins to the support plate with a single flange, and can thus be easily removed without disturbing the connections.

C. A multicell experiment with *magnetic insulation*

The next experiment would be of a multicell magnetically insulated cavity (Fig. 17). This would test the magnetic insulation in a geometry similar to that required in the 201 MHz acceleration for phase rotation or early cooling.

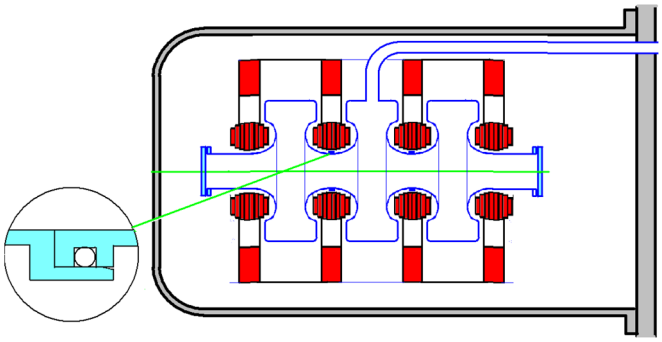

FIG. 17. (Color) Schematic of a multicell cavity with magnetic insulation. The inset shows a possible way to join adjacent cavities inside the solenoid coils.

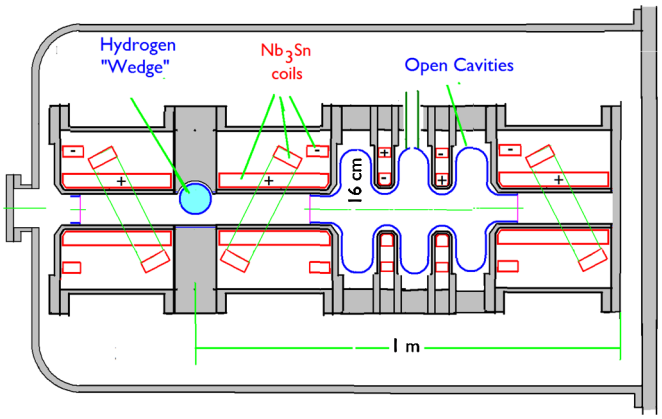

FIG. 18. (Color) Schematic of a lattice for later cooling to lower emittances.

In addition, it would address the problem of joining cavities inside the bore of the solenoids. This joint does not need to carry much rf current, nor does it need to hold high vacuum (since there is vacuum on both sides). The method requiring simple axial pressure is shown in the figure, but other ideas may be explored.

It should be noted that this experiment, and the previous one, test a model of the 201 MHz lattices that would be used in the phase rotation, neutrino factory cooling, and the early cooling in a muon collider.

D. Testing of components for later 6D cooling

Later 6D cooling will require compact higher field (10–15 T) solenoids in order to focus the beams to lower β's and thus cool to lower emittances. Test coils could conveniently be tested on the proposed test stand, since it would allow for easy mounting, cooling, and testing with easily accessible instrumentation. Later, these coils would be used in conjunction with 805 MHz cavities (see Fig. 18). The first stage of the 10–20 T solenoid development could appropriately be tested in the same test stand discussed above. Subsequently, the rf cavities would be included. The final step would be to add the required hydrogen absorber. The details of the lattice would not change the nature of the components needing test. Figure 18 is thus not meant as a definitive design of the required lattice, but rather as a test of the kind of components needed; the cavity shapes shown are not those with true magnetic insulation. The true shapes with their coils are yet to be determined. Figure 18 is thus intended only as an illustration of the direction of the required R&D.

E. Testing of magnetic field solutions at 201 MHz

The experiments already planned with the 201 MHz cavity in several Tesla fields could show satisfactory performance. If however this is not the case, then whatever solutions are proposed on the basis of the 805 MHz tests will need to be demonstrated at 201 MHz.

VI. CONCLUSIONS

A brief review of models for breakdown without external magnetic fields suggests that the initiation of breakdown is best explained by Ohmic heating due to field emission current at asperities. The dependence of breakdown on frequency, pulse length, and cavity materials can be explained by the competing processes of asperity destruction and the creation of new asperities. We have proposed a new model for damage in rf cavities operated in significant axial magnetic fields. The model fits the existing data reasonably well. The model also fits some otherwise surprising results from a pillbox cavity with a Be window facing a Cu plate with a central button. The model predicts relatively low gradient breakdowns at 201 MHz in magnetic fields. These predicted breakdowns occur at significantly lower gradients than the operating gradients specified for the phase rotation and initial cooling in the International Scoping Study (ISS) [1] neutrino factory and in a muon collider. Methods to address these problems are discussed, including the use of *magnetically insulated rf*. A possible experimental program to study this concept is outlined.

ACKNOWLEDGMENTS

We would like to thank J. Norem, A. Moretti, and A. Bross for many discussions and sharing their experimental data. This work has been supported by U.S. Department of Energy under Contracts No. AC02-98CH10886 and No. DE-AC02-76CH03000.

[1] International Scoping Study (ISS), http://www.cap.bnl.gov/mumu/project/ISS/.
[2] R. B. Palmer *et al.*, in *Proceedings of the 2007 Particle Accelerator Conference, Albuquerque, New Mexico, 2007*, edited by C. Petit-Jean-Genaz (IEEE, Albuquerque, New Mexico, 2007), p. 3193.
[3] J. Norem *et al.*, Phys. Rev. ST Accel. Beams **6**, 072001 (2003).
[4] A. Moretti *et al.*, Phys. Rev. ST Accel. Beams **8**, 072001 (2005).
[5] P. Hanlet *et al.*, in *Proceedings of the 10th European Particle Accelerator Conference, Edinburgh, Scotland, 2006* (EPS-AG, Edinburgh, Scotland, 2006), p. 1364; R. Johnson (private communication).
[6] R. H. Fowler and L. Nordheim, Proc. R. Soc. A **119**, 173 (1928).
[7] J. Norem *et al.*, in *Proceedings of the 20th Particle Accelerator Conference, Portland, OR, 2003*, edited by J. Chew, P. Lucas, and S. Webber (IEEE, Piscataway, NJ, 2003), p. 1246.
[8] G. A. Loew and J. W. Wang, SLAC Report No. SLAC-PUB-4647, 1988; and again proposed for high pressure gas filled cavities, R. Johnson (private communication).
[9] P. Wilson, SLAC Report No. SLAC-PUB-7449, 1997.
[10] P. Wilson, SLAC Report No. SLAC-PUB-9953, 2003; in Proceedings of the Workshop on High Gradient RF; ANL (2003); P. Wilson *et al.*, in Proceedings of LINAC04, Lubeck, Germany, 2004, p. 189.
[11] R. Siemann, SLAC Report No. SLAC-PUB-7449, SLAC SLAC-TN-05-086, ARDB122, 1997; see also Ref. [9]; J. W. Wang and G. A. Loew, SLAC Report No. SLAC-PUB-7684, 1997.
[12] S. Döbert, Power Modulator Symposium, 2004 and 2004 High-Voltage Workshop. Conference Record of the 26th International, 2004, pp. 60–63; W. Wuensch, in *Proceedings of the 8th European Particle Accelerator Conference, Paris, 2002* (EPS-IGA and CERN, Geneva, 2002).
[13] V. A. Dolgashev and S. G. Tantawi, in Proceedings of the 8th European Particle Accelerator Conference, Paris, 2002 (Ref. [12]), p. 2139.
[14] J. Norem *et al.*, Recent rf results from the Mucool Test Area, in Proceedings of the 2007 Particle Accelerator Conference, Albuquerque, New Mexico, 2007 (Ref. [2]), pp. 2239–2241.
[15] D. Li *et al.*, in *Proceedings of the NuFact07 Workshop*, AIP Conf. Proc. 981 (AIP, New York, 2008), pp. 299–302.
[16] A. Moretti, MTA RF 201 MHz operations update, presentation at NFMCC Friday Meeting, 2008; http://www.fnal.gov/projects/muon_collider/FridayMeetings.
[17] A. Hassanein *et al.*, Phys. Rev. ST Accel. Beams **9**, 062001 (2006).
[18] D. Huang, Fermilab MTA 805 MHz Program, MUTAC, 2008; http://www.cap.bnl.gov/mumu/conf/MUTAC-080408/talks/09AM/DHuang1-080408.pdf.
[19] D. Huang, Recent update of 805 MHz cavity material test, NFMCC Friday Meeting, 2008, http://www.fnal.gov/projects/muon_collider/FridayMeetings/23-MAY-2008/Huang.ppt; D. Huang *et al.*, Report No. MUC-525, 2008.
[20] A. Tollestrup, in the 3rd LEMC Workshop, FNAL, 2008, http://www.muonsinc.com/lemc2008/presentations/alvin_BeamGasCavityLEworkshopFNAL4_22_08.ppt.
[21] R. Fernow, NFMCC Technical Note 533, 2009, http://nfmcc-docdb.fnal.gov/cgi-bin/DocumentDatabase/.
[22] J. H. Billen and L. M. Young, SUPERFISH, Los Alamos National Laboratory Report No. LA-UR-96-1834, 1996.
[23] W. D. Kilpatrick, Rev. Sci. Instrum. **28**, 824 (1957); G. A. Loew and J. W. Wang, *Handbook of Accelerator Physics and Engineering*, edited by A. W. Chao and M. Tigner (World Scientific, Singapore, 1999), p. 390.
[24] MICE, http://www.mice.iit.edu/.
[25] K. Kanaya and S. Okayama, J. Phys. D **5** 43 (1972); J. Wittke, Electron Microprobe Notes, http://www4.nau.edu/microanalysis/Microprobe/Probe.html.
[26] J. Norem; Recent Results of High Gradient Studies at Argonne, http://www.fnal.gov/projects/muon_collider/FridayMeetings/11-JAN-2008/Norem.pdf.
[27] F. Winterberg, Rev. Sci. Instrum. **41**, 1756 (1970); **43**, 814 (1972).
[28] A. Moretti, at the 2008 NFMCC Collaboration Meeting, Fermilab 2008, http://www.cap.bnl.gov/mumu/conf/MC-080317/talks/AMoretti1-080317.pdf.
[29] J. Norem *et al.* (private communication).
[30] A. Moretti *et al.*, in Proceedings of LINAC04, p. 271 (2004).